

## Spin Dependent Tunneling and Magnetoresistance in Magnetic Granular Systems with Coulomb Blockade

Saburo TAKAHASHI and Sadamichi MAEKAWA

*Institute for Materials Research, Tohoku University, Sendai 980-8577, Japan*

(Received October 27, 1999)

We theoretically study the magnetoresistance (MR) in a magnetic granular system containing nanoscale ferromagnetic granules in an insulating matrix. Taking account of spin-dependent tunneling and Coulomb blockade in the granular structure, we calculate the temperature as well as bias voltage dependence of magnetoresistance (MR). The MR is anomalously enhanced at low temperatures due to successive onset of higher-order tunneling processes between larger granules through intervening smaller ones. The enhanced MR at low temperatures is maintained up to high bias voltages. Both temperature and bias-voltage dependence of the MR are in good agreement with recent experiments in Co-Al<sub>2</sub>O<sub>3</sub> granular films.

KEYWORDS: granular materials, giant magnetoresistance, spin-dependent tunneling, Coulomb blockade

### §1. Introduction

Magnetotransport phenomena in magnetic nanostructures have attracted much attention since the discovery of giant magnetoresistance (GMR) in magnetic multilayers.<sup>1)</sup> In addition, there is a growing interest in the study of magnetoresistive phenomena in ferromagnetic tunnel junctions;<sup>2-5)</sup> this has led to new research work in tunnel-type magnetic nanostructures such as granular films containing ferromagnetic granules in a insulating matrix<sup>6-14)</sup> and ferromagnetic multi-tunnel junctions.<sup>15-27)</sup> Of particular interest in such magnetic nanostructures is not only to find new phenomena due to nanostructuring but also applications to magnetoresistive devices.

In the tunnel-type magnetic nanostructures, the electrical conduction is caused by tunneling of electrons across insulating barriers. The magnetotransport properties are dominated by the following effects. First, tunneling current between ferromagnetic granules or electrodes depends on the relative orientation of the magnetic moments (spin-dependent tunneling).<sup>2,3)</sup> The tunnel resistance decreases when the magnetic moments are aligned parallel to the direction of applied magnetic field. Second, tunneling electron into small granules increases the Coulomb charging energy,<sup>28)</sup> which opens the Coulomb gap and strongly enhances the tunnel resistance at low temperatures (Coulomb blockade).<sup>29)</sup> Therefore, we expect novel magnetoresistive phenomena by the interplay of the two effects coexisting in the tunnel-type magnetic nanostructures.

Magnetic granular materials containing ferromagnetic granules of nanometer size in an insulating matrix are unique systems, since the magnetic moments of the granules are randomly oriented, and the charging energy  $E_c$  of the granules is broadly distributed due to the variation of granule size  $d$  ( $E_c \sim e^2/d$ ). The conduction of charge carriers in the granular structures involves a large number of Co granules with different size. Once a

charge carrier enters a large granule, which is surrounded by smaller ones, the carrier cannot tunnel to the neighboring small granules due to the Coulomb blockade at low temperatures. However, because of the distribution of granule size, the carrier can find a large granule of nearly equal size in the neighborhood, which is separated by a number of small granules. Then, it is energetically allowed to transfer the carrier through the intervening small granules to the large granule using the higher order tunneling process, where several successive tunneling processes of single electrons are involved in the intermediate state (Fig. 1). The successive tunneling is much easier in aligned magnetic moments in a high magnetic field than in randomly oriented ones in zero field. Therefore, we expect a large enhancement of MR due to the higher order tunneling process.

In this paper, we study the magnetoresistive properties of tunnel-type granular systems with spin-dependent tunneling and Coulomb blockade. We calculate the resistivity and the MR as functions of temperature and bias-voltage. We find that the MR exhibits an anomalous increase in the temperature dependence and attains large enhanced values at low temperatures, and that the enhanced MR is maintained to high bias-voltages. The large enhancement of the MR originates from higher-order processes in the spin-dependent tunneling between large granules through intervening small ones in the Coulomb blockade regime. The existence of higher-order tunneling processes in granular systems is a consequence of their granular structure with broad distribution of granule size.

### §2. Model for the granular systems

We describe a model for magnetic granular systems which provides a consistent explanation for the temperature and bias-voltage dependence of the resistivity and the MR observed in Co-based granular films.

The characteristic temperature dependence of the elec-

trical resistivity,  $\ln \rho_0(T) \propto 1/\sqrt{T}$ , has been observed in magnetic as well as nonmagnetic granular materials in a wide range of metal-nonmetal compositions below the percolation threshold. Sheng *et al.*<sup>28)</sup> have derived the temperature dependence based on the model that granules on each conduction path are equal in size  $d$  and separated by barrier thickness  $s$ , keeping their ratio  $s/d$  (or equivalently  $E_c s$ ) constant for a given composition. In this model, the electrical conductivity  $\sigma_0(T)$  at high temperatures is contributed from tunneling between small granules, while at low temperatures  $\sigma_0(T)$  is from tunneling between large granules. An extension to the magnetic granular systems has been made by Inoue and Maekawa,<sup>30)</sup> who incorporate the effect of spin-dependent tunneling into the model and obtain the spin-dependent conductivity  $\sigma_m(T) = (1 + P^2 m^2) \sigma_0(T)$  and the MR ratio

$$\Delta\rho/\rho_0 = P^2 m^2 / (1 + P^2 m^2), \quad (2.1)$$

where  $P$  is the spin-polarization of the granules and  $m = M/M_s$  the magnetization normalized to the saturation magnetization  $M_s$ . The  $m = 0$  ( $m = 1$ ) correspond to the randomly (fully) oriented magnetic moments of granules in zero (high) magnetic field. The formula (2.1) reproduces well the behavior of  $\Delta\rho/\rho_0 \propto m^2$  observed in magnetic granular systems.<sup>6)</sup>

Recently, Mitani *et al.*<sup>10)</sup> have found that the MR in Co-based granular films exhibits a strong temperature dependence at low temperatures and is enhanced more than 20 % at 4.2 K, which is twice as large as the value of 11 % estimated from Eq. (2.1) using  $P = 0.34$  for Co.<sup>31)</sup> It should be noted that the above model makes a gross simplification for the actual conduction paths by neglecting tunneling between granules of unequal size. We extend the model to include tunneling between those granules, which plays a crucial role for the MR in the magnetic granular systems.

In the granular systems with a broad distribution of granule size, large granules are distant from each other due to their low number density, i.e., the larger the granule size is, the more separated the granules are, so that there is a number of smaller granules between large granules as shown in Fig. 1(a). For modeling the structural feature of granular systems, we assume that, when there are large granules with size  $n\bar{d}$  and charging energy  $\bar{E}_c/n$ , they are separated by the number of  $n$  intervening granules with the average size  $\bar{d}$  and charging energy  $\bar{E}_c$ , as shown in Fig. 1(b). The tunneling distance between the neighboring granules is  $s' = 2n\bar{s}/(n+1)$ , where  $\bar{s}$  is a mean separation if all the granules would have the average size  $\bar{d}$ .

### §3. Temperature dependence of MR

We calculate the temperature dependence of the conductivity  $\sigma_m(T)$  at zero bias voltage ( $V = 0$ ) in our model structure of granular systems. The tunneling current in the zero bias limit is dominated by thermally activated charge carriers. In the conduction path in Fig. 1(b), the carriers occupy mostly the large granule

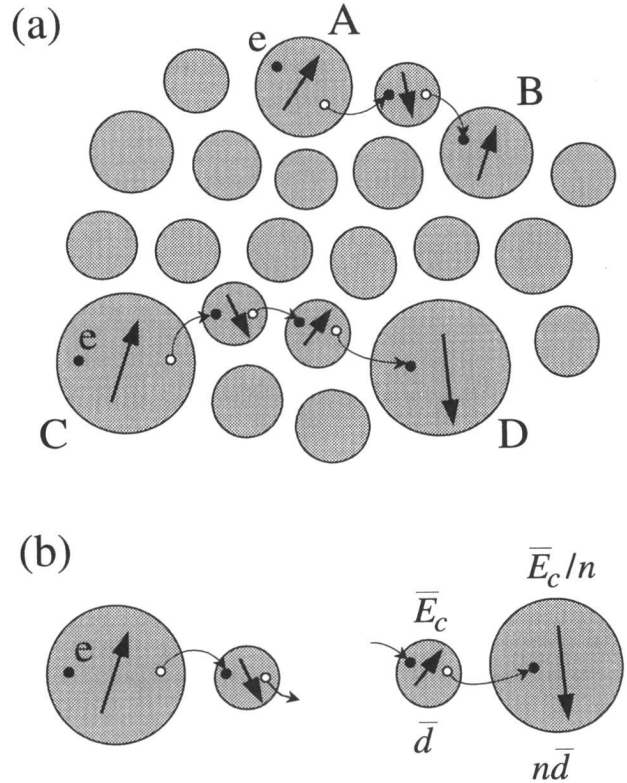


Fig. 1. (a) Schematic diagram of granular structure and a higher order tunneling process where a charge carrier is transferred from the charged large granule A (C), via the small ones, to the neutral large one B (D), leaving behind an electron and a hole excitation on the granules. (b) Conduction path used for the calculation of the electrical conductivity.

of charging energy  $\bar{E}_c/n$ <sup>32)</sup> in the probability proportional to the Boltzmann factor  $\exp[-\bar{E}_c/2nk_B T]$ . Since the charged large granules are separated by the smaller granules, the ordinary tunneling of an electron from the large granule to the small granule causes an increase of charging energy  $\delta E_c \sim 1/(1+1/n)\bar{E}_c$ , the difference in the charging energies between the large and small granules, and thus is suppressed by the Coulomb blockade at low temperatures ( $k_B T \ll \delta E_c$ ). In this regime, the dominant contribution to  $\sigma_m(T)$  comes from higher order tunneling processes where the carrier is transferred to the neighboring large granule through the intervening small ones using the successive tunneling of single electrons, i.e., the cotunneling of  $(n+1)$  electrons, leaving behind an electron and a hole excitation in each granule (see Fig. 1(b)).

In the higher-order process, the total probability of the spin-dependent tunneling between the large granules is given by the product of those between the neighboring granules:

$$\left\langle \prod_{i=0}^n e^{-2\kappa s'} (1 + P^2 \cos \theta_{i,i+1}) \right\rangle, \quad (3.1)$$

where  $\kappa$  is the tunneling parameter related to the barrier height and width,  $\theta_{i,i+1}$  is the angle between the magnetic moments  $\vec{\mu}_i$  and  $\vec{\mu}_j$  of the neighboring granules  $i$

and  $i+1$ , and  $\langle \dots \rangle$  denotes the average over the direction of the magnetic moments. If we expand Eq. (3.1) with respect to  $P^2$  up to the first order and use the relation

$$\langle \cos \theta_{i,i+1} \rangle = \frac{\langle \vec{\mu}_i \cdot \vec{\mu}_j \rangle}{\mu_i \mu_j} = m^2, \quad (3.2)$$

we obtain  $[1 + (n+1)P^2m^2]e^{-4\kappa n\bar{s}} + O(P^4)$ . Taking account of the fact that Eq. (3.1) gives  $(1+P^2)^{n+1}e^{-4\kappa n\bar{s}}$  in the high field limit where  $\cos \theta_{i,i+1} = 1$ , we may write Eq. (3.1) in the form  $(1+P^2m^2)^{n+1}e^{-4\kappa n\bar{s}}$  valid for  $P^2 \ll 1$ .

Summing up all of the higher-order processes of the spin-dependent tunneling, we obtain the zero bias conductivity

$$\sigma_m(T) \propto \sum_n (1+P^2m^2)^{n+1} e^{-4\kappa n\bar{s}} e^{-\bar{E}_c/2nk_B T} \times \left[ \frac{(\pi k_B T)^2}{(\delta E_c)^2 + \gamma^2(T)} \right]^{2n} f(n). \quad (3.3)$$

Here, the factor  $[\dots]^{2n}$  originates from the electron and hole excitations in the energy interval  $\pi k_B T$  around the Fermi level in the intermediate state,<sup>33,34</sup> and  $\gamma(T)$  is the decay rate given by the high temperature form  $\gamma(T) \sim gk_B T$  with  $g$  being a constant.<sup>35</sup> The function  $f(n)$  represents a distribution of the conduction paths. In Eq. (3.3), the exponential factor  $\exp[4\tilde{\kappa}n\bar{s} - \bar{E}_c/2nk_B T]$ , where the factor  $[\dots]^n$  is included, has a sharp peak at  $n = n^*$ :

$$n^* = \left( \frac{\bar{E}_c}{8\tilde{\kappa}\bar{s}k_B T} \right)^{1/2}, \quad (3.4)$$

where  $\tilde{\kappa}$  is the effective tunneling parameter given by

$$\tilde{\kappa}/\kappa \simeq 1 + \frac{1}{4\kappa\bar{s}} \ln \left[ \frac{\gamma^2(T) + \bar{E}_c^2}{(\pi k_B T)^2} \right]. \quad (3.5)$$

At low temperatures ( $k_B T \ll \bar{E}_c$ ),  $n^*$  becomes large so that  $n$  is treated as a continuous valuable. Replacing the summation by the integration and using the method of steepest descent in Eq. (3.3), we obtain the spin-dependent conductivity

$$\sigma_m(T) = (1+P^2m^2)^{n^*+1} \sigma_0(T), \quad (3.6)$$

with the spin-independent conductivity

$$\sigma_0(T) \propto \left( \frac{k_B T}{2\tilde{\kappa}\bar{s}\bar{E}_c} \right)^{1/4} \exp \left[ -2 \left( \frac{2\tilde{\kappa}\bar{s}\bar{E}_c}{k_B T} \right)^{1/2} \right], \quad (3.7)$$

where we assume  $f(n^*) \propto 1/n^*$ .<sup>36</sup> At low temperatures, the exponential factor in Eq. (3.7) gives the dominant contribution to the temperature dependence of  $\sigma_0(T)$ . Since  $\tilde{\kappa}$  depends weakly on temperature only logarithmically, the resistivity  $\rho_0(T) = 1/\sigma_0(T)$  nearly follows the relation  $\ln \rho_0(T) \propto 1/\sqrt{T}$ .

Figure 2 shows the resistivity  $\rho_0(T)$  in zero field ( $m = 0$ ). In the calculation, and take the values of the parameters:  $2\kappa\bar{s} = 3.5$ ,  $g = 0.3$ , and  $\bar{E}_c = 100$  K. It is seen that the curve slightly deviates from the straight line, i.e., the relation  $\ln \rho_0(T) \propto 1/\sqrt{T}$ , exhibiting a small upturn cur-

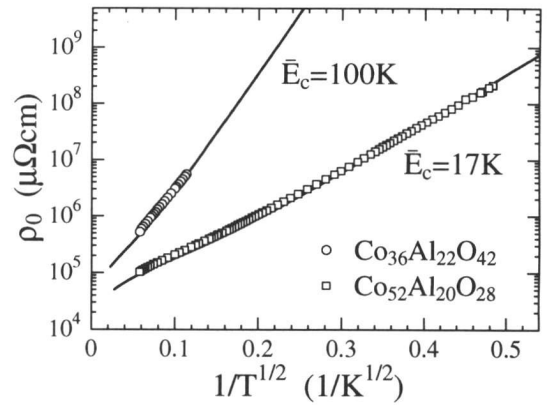


Fig. 2. Temperature dependence of  $\rho_0(T)$  vs  $1/T^{1/2}$  for with the charging energy of  $\bar{E}_c = 100$  K and  $\bar{E}_c = 17$  K. The circles and squares represent the experimental data of  $\text{Co}_{36}\text{Al}_{22}\text{O}_{42}$  and  $\text{Co}_{52}\text{Al}_{20}\text{O}_{28}$  granular films measured by Mitani *et al.*<sup>10</sup>

vature. This upturn results from a weak temperature dependence of  $\tilde{\kappa}$  in the exponential factors of Eq. (3.7). Our model reproduces the resistivity of  $\text{Co}_{36}\text{Al}_{22}\text{O}_{42}$  granular films.<sup>10</sup>

Due to the higher order processes, the spin-dependent part of  $\sigma_m(T)$  in Eq. (3.6) is amplified to the  $(n^*+1)$ th power of  $(1+P^2m^2)$ , so that the resistivity  $\sigma_m(T)$  is sensitive to the change of  $m$  by application of magnetic field. Substituting Eq. (3.6) into the MR ratio defined by

$$\Delta\rho/\rho_0 = [\rho_0(T) - \rho_m(T)]/\rho_0(T), \quad (3.8)$$

we have the MR ratio in the granular systems

$$\Delta\rho/\rho_0 = 1 - (1+m^2P^2)^{-(n^*+1)}. \quad (3.9)$$

The MR ratio has rather a simple form because of the cancellation of  $\sigma_0(T)$ , which is the complicated function of temperature and granular structure, is dropped out by taking the ratio.

Figure 3 shows the MR ratio for  $m = 1$  and  $P = 0.31$ . The value of  $P$  is slightly smaller than that of  $\text{Co} = 34\%$  measured by tunnel spectroscopy.<sup>31</sup> Other parameters are the same as those in Fig. 2. The solid dots represent the experimental data of  $\text{Co}_{36}\text{Al}_{22}\text{O}_{42}$  by Mitani *et al.* The dashed line indicates the value of the MR ratio in Eq. (2.1). For small  $P^2$ , Eq. (3.9) is approximated to be a convenient formula

$$\Delta\rho/\rho_0 \approx P^2m^2 \left( 1 + \sqrt{C/T} \right), \quad (3.10)$$

with  $C (= \bar{E}_c/8\tilde{\kappa}\bar{s}k_B)$  being a constant. The dashed curves in Fig. 3 indicate the values calculated from the formula (3.10) for  $m = 1$ ,  $P = 0.325$ , and  $C = 2.6$  K. The anomalous increase of  $\Delta\rho/\rho_0 \sim 1/\sqrt{T}$  at low temperatures is due to the onset of higher order processes between larger granules, i.e.,  $n^* \propto 1/\sqrt{T}$ . As seen in the curve, the MR grows rapidly around  $\sim 10$  K well below  $\bar{E}_c = 100$  K. Similar behavior is seen in a ferromagnetic single-electron tunneling transistor (SET).<sup>22,23</sup> At high temperatures ( $k_B T \gg \bar{E}_c$ ), Eq. (3.9) reproduces the for-

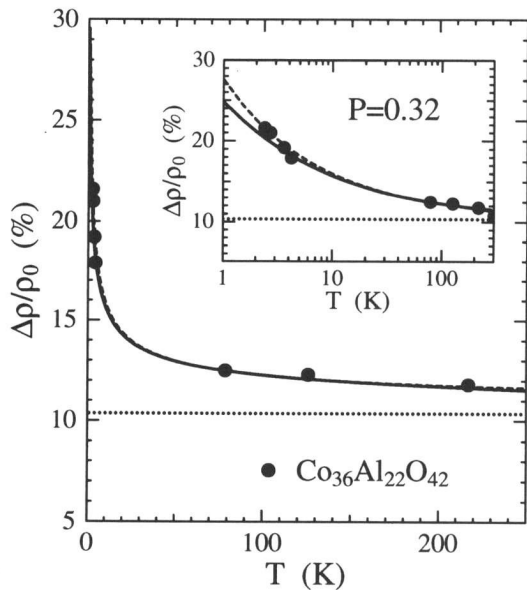


Fig. 3. Temperature dependence of MR calculated from Eq. (3.9) with the spin-polarization  $P = 0.32$ . Other parameters are the same as those in Fig. 2. The dashed curve indicates the MR ratio calculated from the formula  $\Delta\rho/\rho_0 = P^2 [1 + (C/T)^{1/2}]$  with  $P = 0.325$  and  $C = 2.6$  K. The dotted line indicates the MR ratio  $P_{Co}^2/(1 + P_{Co}^2)$  in the absence of Coulomb blockade. The solid dots represent the experimental data of  $\text{Co}_{36}\text{Al}_{22}\text{O}_{42}$  granular films by Mitani *et al.*<sup>10)</sup>

mula (2.1) in the absence of the charging effect.

#### §4. Bias voltage dependence of MR

We next calculate the bias-voltage ( $V$ ) dependence of the conductivity  $\sigma_m(V)$  at low temperatures. In the Coulomb blockade regime, where the thermally-activated carriers are dominated over those generated by the bias voltage, the  $V$ -dependence of  $\sigma_m$  at  $T = 0$  is obtained if the factor  $(\pi k_B T)^{2n}$  in Eq. (3.3) is replaced with the factor  $(e\Delta V)^{2n}/(2n)! \simeq (e\Delta V/n)^{2n} = (2eV/N_g)^{2n}$ ,<sup>33,34)</sup> where  $\Delta V$  is the voltage drop between the large granules and is related to  $V$  by  $\Delta V = (2n/N_g)V$ , and  $N_g$  is the average number of granules along a conduction path between electrodes. At finite temperatures, we use the interpolation formula  $[(\pi k_B T)^2 + (2eV/N_g)^2]^n$  for the factor. Making use of these replacements, we derive  $\sigma_m(V)$  whose expression is the same as that in Eq. (3.3) if  $\tilde{\kappa}$  reads

$$\tilde{\kappa}/\kappa \simeq 1 + \frac{1}{4\kappa s} \ln \left[ \frac{\gamma^2(T) + \bar{E}_c^2}{(\pi k_B T)^2 + (2eV/N_g)^2} \right]. \quad (4.1)$$

For  $2\kappa s \gg 1$ ,  $\sigma_m(V)$  reduces to

$$\sigma_m(V) = \sigma_m(T) \left[ 1 + \left( \frac{2eV}{\pi N_g k_B T} \right)^2 \right]^{n_0^*}, \quad (4.2)$$

where  $\sigma_m(T)$  is given by Eq. (3.6) and  $n_0^* = (\bar{E}_c/8\kappa s k_B T)^{1/2}$ . The  $\sigma_m(V)$  exhibits a power law dependence  $(1/V)^{2n_0^*}$  for  $k_B T < eV/N_g < \bar{E}_c$ . Note that the conductance of SET behaves as  $1/V^2$  in the Coulomb

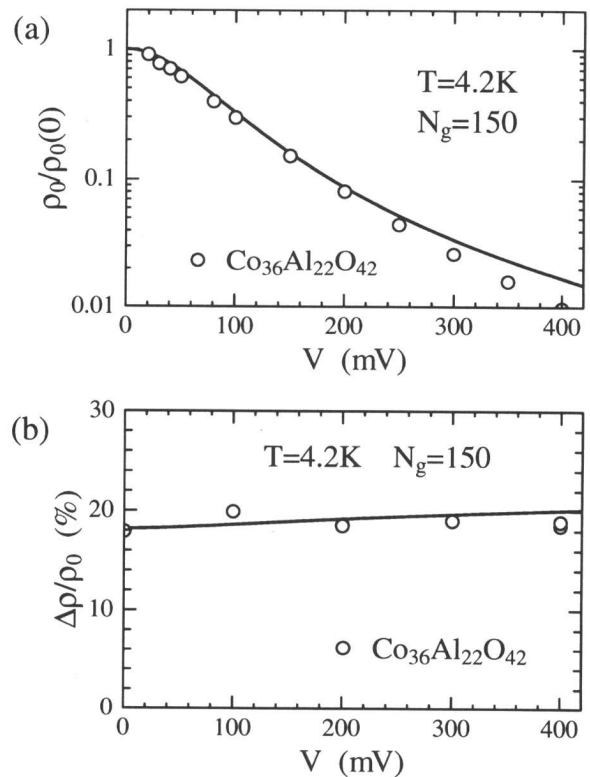


Fig. 4. Bias dependence of (a) resistivity  $\rho_0(V)$  and (b) MR ratio  $\Delta\rho/\rho_0$ . The parameters are the same as those in Fig. 2. The open circles indicate the experimental results of  $\text{Co}_{36}\text{Al}_{22}\text{O}_{42}$  film at 4.2 K.<sup>10)</sup>

blockade regime.<sup>33)</sup>

Figure 4(a) show the resistivity  $\rho_0(V) = 1/\sigma_0(V)$  calculated from Eq. (4.2) for  $T = 4.2$  K and  $N_g = 150$ . The value of  $N_g = 150$  is somewhat smaller than the value  $200 \sim 300$  estimated from the image of TEM micrographs.<sup>37)</sup> The calculated resistivity decreases steeply with increasing  $V$ , in agreement with the experimental data. A deviation of the calculated values from the experimental ones starts at about 300 meV and increases at higher voltages, suggesting that the charge carriers generated by the bias voltage, which is neglected in the present paper, have a significant contribution to the tunneling current in the high voltage regime.

The  $V$ -dependence of the MR ratio is also given by Eq. (3.9) if Eq. (4.1) is used for  $\tilde{\kappa}$  in  $n^*$ . Figure 4(b) shows the  $V$ -dependence of the MR ratio. The enhanced MR ratio is maintained up to higher voltages, in agreement with the experimental data of  $\text{Co}_{36}\text{Al}_{22}\text{O}_{42}$ . This is because the MR ratio depends only logarithmically on the voltage drop  $\Delta V \sim V/N_g$  between neighboring granules. The almost constant MR originates from the large number of granules along the conduction paths in the granular films. The voltage drop  $\Delta V$  is about 3 mV for  $N_g = 150$  and  $V = 400$  mV, and its corresponding temperature is  $\sim 30$  K, which is smaller than the charging energy  $\bar{E}_c \sim 100$  K. The gradual increase of the calculated MR at higher voltages reflects the weak  $V$ -dependence of  $\tilde{\kappa}$ . We note that the enhanced MR is nearly constant up to 500 meV, whereas the correspond-

ing resistance is reduced by several orders of magnitude. This is in contrast with ferromagnetic tunnel junctions with macroscopic size, where both MR and resistance decrease gradually with increasing bias-voltage.<sup>5)</sup>

We discuss the origin of the different behavior in the  $T$  and  $V$  dependence of the MR. For small  $P^2$ , Eq. (3.9) is approximated as  $\Delta\rho/\rho_0 \approx (1 + n^*)P^2m^2$ , implying that the MR is directly related to the order of dominating tunneling process  $(1 + n^*)$  at given temperature. As seen in the derivation of Eq. (3.7), the singular behavior  $n^* \sim 1/\sqrt{T}$  stems from the strongly temperature dependent Boltzmann factor that determines the carrier distribution on the granules of different size (i.e., different charging energy). As the temperature is lowered below  $\bar{E}_c$ , the thermally activated carriers that contribute to the conductivity decrease exponentially and distribute selectively on large granules with smaller charging energy, so that the order of tunneling process increases rapidly to the higher order with decreasing temperature. On the other hand, the bias voltage  $V$  does not affect directly the distribution of the carriers. In addition, a large number of granules is contained along the conduction paths in the granular films, so that the voltage drop between neighboring granules  $\sim V/N_g$  remains to be smaller than the charging energy  $E_c$ . Therefore the granular films shows almost no  $V$ -dependence in the MR.

### §5. Tunnel junction with granules in the barrier

There has been a number of experiments on ferromagnetic tunnel junctions in which ferromagnetic granules such as Co are dispersed in the insulating layer of the tunnel barrier.<sup>16-20)</sup> In these hybrid tunnel junctions, thermodynamical fluctuations in the direction of magnetic moments of granules, i.e., superparamagnetism, is seen in the higher-order process of the spin-dependent tunneling. To demonstrate this, we consider a tunnel junction containing a small granule in the barrier as shown in Fig. 5. The magnetic moments of the electrodes take either ferromagnetic (F) or antiferromagnetic (AF) alignment. The magnetic moment of the granule is in a superparamagnetic state, i.e., thermally rotating in zero applied magnetic field. In the Coulomb blockade regime  $k_B T \ll E_c$ , the current is dominated by the cotunneling through the granule. Using the spin-dependent tunneling probability in Eq. (3.1) with  $n = 1$ , the conductance  $G_F(H)$  in the F alignment is written as

$$G_F(H) = G_0(T) [1 + 2P^2\langle\cos\theta\rangle + P^4\langle\cos^2\theta\rangle], \quad (5.1)$$

while in the AF alignment

$$G_{AF}(H) = G_0(T) [1 - P^4\langle\cos^2\theta\rangle], \quad (5.2)$$

where  $\theta$  is the angle between the moment of the left electrode and the granule and  $\langle\cdots\rangle$  denotes the thermal average. The  $\langle\cos\theta\rangle$  represents the polarization of the moment  $\mu_g$  in the direction of  $H$  and is given by the Langevine function  $L(x)$ :

$$\langle\cos\theta\rangle = L(x) = \coth(x) - 1/x, \quad x = \mu_g H/k_B T. \quad (5.3)$$

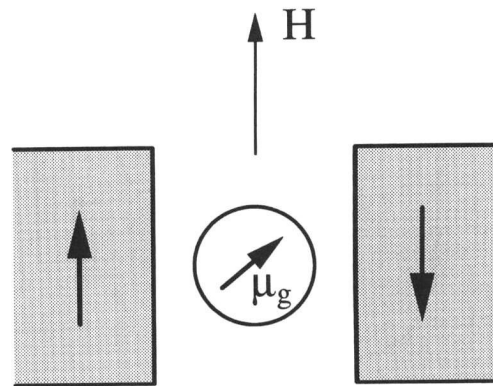


Fig. 5. Tunnel junction containing a small granule in the insulating barrier. The magnetic moment of the granule is in a superparamagnetic state, i.e., thermally rotating, and those of the left and right electrodes take either ferromagnetic (F) or antiferromagnetic (AF) alignment.

The term  $\langle\cos^2\theta\rangle$  appears as a consequence of the cotunneling process and is given by

$$\langle\cos^2\theta\rangle = 1 - (2/x)L(x), \quad (5.4)$$

which represents the correlation between the moments. This enables us to extract the thermal fluctuation of the moment  $\mu_g$  by measuring the conductance (or resistance) in the Coulomb blockade regime.

In zero field ( $H = 0$ ), the magnetic moments are randomly oriented, where  $\langle\cos\theta\rangle = 0$  and  $\langle\cos^2\theta\rangle = 1/3$ , so that

$$G_F(H) = G_0(T) [1 + P^4/3], \quad (5.5)$$

in the F alignment, while

$$G_{AF}(H) = G_0(T) [1 - P^4/3], \quad (5.6)$$

in the AF alignment. Therefore the cotunneling gives rise to the difference in the conductance at  $H = 0$ , and the resistance ratio is given by

$$(R_{AF}/R_F)_{H=0} \approx 1 + (2/3)P^4. \quad (5.7)$$

Figure 6(a) shows the resistance,  $R_F(H)$  and  $R_{AF}(H)$ , as a function of magnetic field  $H$  for the spin-polarization  $P = 50\%$  in the electrodes and the granule. Figure 6(b) shows the  $H$ -dependence of the resistance obtained from the curves in Fig. 6(a), when the magnetic moments of the electrodes are in the AF alignment for fields  $|H|$  between 100 Oe and 300 Oe and otherwise in the F alignment. Here, we assume  $\mu_g = 1000\mu_B$  for the magnetic moment of the granule and take  $T = 67$  K for temperature, yielding a scale of magnetic field  $k_B T/\mu_g = 1$  kOe for a thermally rotating granule. The resistance curve in Fig. 6(b) is similar to that of recent experiments in hybrid junctions.<sup>17,18)</sup>

### §6. Summary

We have shown that the higher order tunneling in the spin-dependent tunneling with the Coulomb block-

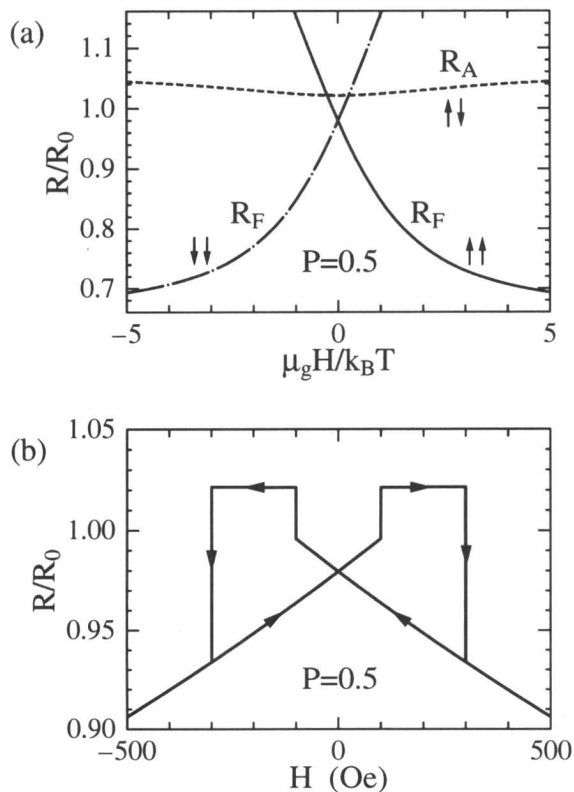


Fig. 6. (a) Resistance  $R_F(H)$  and  $R_{AF}(H)$  as a function of magnetic field  $H$ . (b) Resistance curve obtained from the curves in (a) when the magnetic moments of the electrodes are parallel for fields  $|H|$  between 100 Oe and 300 Oe and antiparallel otherwise.

ade plays an important role in the magnetoresistive phenomena of the magnetic granular systems. The rapid increase of the MR at low temperatures is interpreted as the progressive onset of higher order tunneling between larger granules in magnetic granular system. The temperature and bias-voltage dependence of the resistivity and the MR ratio explain consistently the experimental results.

### Acknowledgements

We are grateful to S. Mitani, H. Imamura, K. Takanashi, J. Inoue, P.M. Levy, and H. Fujimori for fruitful discussions. This work is supported by a Grant-in-Aid for Scientific Research Priority Area for Ministry of Education, Science and Culture of Japan, the Grant from Japan Society for the Promotion of Science, CREST and NEDO.

- 1) M. N. Baibich, J. M. Broto, A. Fert, F. Nguyen Van Dau, F. Petroff, P. Etienne, G. Creuzet, A. Friederich, and J. Chazelas: Phys. Rev. Lett., **61** (1988) 2472.
- 2) M. Julliere: Phys. Lett. **54A** (1975) 225.
- 3) S. Maekawa and U. Gäfvert: IEEE Trans. Magn. Mag. **18** (1982) 707.
- 4) T. Miyazaki and N. Tezuka: J. Mag. Mag. Mater. **139** (1995)

- L231.
- 5) J.S. Moodera, L. R. Kinder, T. M. Wong, and R. Meservey: Phys. Rev. Lett. **80** 2941 (1998).
- 6) H. Fujimori S. Mitani, and S. Ohnuma: Mat. Sci. Eng. **B31** (1995) 219.
- 7) A. Milner, A. Gerber, B. Groisman, M. Karpovsky, and A. Gladkikh: Phys. Rev. Lett. **76** (1996) 475.
- 8) T. Furubayashi and I. Nakatani: J. Appl. Phys., **79** (1996) 6285.
- 9) S. Honda, T. Okada, M. Nawate, and M. Tokumoto: Phys. Rev. B **56** (1997) 14566.
- 10) S. Mitani, S. Takahashi, K. Takanashi, K. Yakusiji, S. Maekawa, and H. Fujimori: Phys. Rev. Lett. **81** (1998) 2799.
- 11) S. Mitani, K. Takanashi, K. Yakushiji, and H. Fujimori: J. Appl. Phys. **83** 81998) 6524.
- 12) S. Mitani, H. Fujimori, K. Takanashi, K. Yakushiji, J.G. Ha, S. Takahashi, S. Maekawa, S. Ohnuma, N. Kobayashi, T. Matsumoto, M. Ohnuma, and K. Hono: J. Mag. Mag. Mater. **198-199** (1999) 179.
- 13) T. Zhu and Y. J. Wang: Phys. Rev. B **60**, 11918 (1999).
- 14) H. Imamura, J. Chiba, S. Mitani, K. Takanashi, S. Takahashi, S. Maekawa, and H. Fujimori: Phys. Rev. B **60**, No.22 (1999).
- 15) K. Ono, H. Shimada, and Y. Ootuka: J. Phys. Soc. Jpn. **66** (1997) 1261; *ibid.* **67** (1998) 2852.
- 16) L. F. Schelp, A. Fert, F. Fettar, P. Holody, S. F. Lee, J. L. Maurice, F. Petroff, and A. Vaurés: Phys. Rev. B **56** (1997) R5747.
- 17) K. Inomata, H. Ogiwara, Y. Saito, K. Yusu, and K. Ichihara: Jpn. J. Appl. Phys. **36** (1997) 1380.
- 18) K. Inomata and Y. Saito: Appl. Phys. Lett. **73** (1998) 1143.
- 19) H. Kubota, Y. Fukumoto, S. Thamrongsing, Y. Ando, T. Miyazaki, and C. C. Yu: J. Appl. Phys. **87** (2000).
- 20) K. Ono, E. Kita, C. Yasui, K. Asami, and H. Yanagihara: J. Magn. Soc. Jpn. **23** (1999).
- 21) J. Barnas and A. Fert: Phys. Rev. Lett. **80** (1998) 1058.
- 22) S. Takahashi and S. Maekawa: Phys. Rev. Lett. **80** (1998) 1758.
- 23) S. Takahashi and S. Maekawa: J. Magn. Magn. Mater. **197** (1999) 143.
- 24) A. Brataas, Yu. V. Nazarov, J. Inoue, and G. E. W. Bauer: Phys. Rev. B, **59** (1999) 93; Eur. Phys. J. B. **9** (1999) 421.
- 25) J. Inoue, A. Brataas, Yu. V. Nazarov, and G. E. W. Bauer: Surface Sci. **438** (1999) 336.
- 26) H. Imamura, S. Takahashi, and S. Maekawa: Phys. Rev. B **59** (1999) 6017.
- 27) S. Takahashi, H. Imamura, and S. Maekawa: Phys. Rev. Lett. **82** (1999) 3911; J. Appl. Phys. **87** (2000) in press.
- 28) B. Abeles, P. Sheng, M. D. Coutts, and Y. Arei: Adv. Phys. **24** (1975) 407.
- 29) See, for example, *Single Charge Tunneling*, edited by H. Grabert and M.H. Devoret, (Plenum Press, Ney York, 1992).
- 30) J. Inoue and S. Maekawa: Phys. Rev. B **53** (1996) R11927.
- 31) R. Meservey and P. M. Tedrow: Phys. Rep. **38** (1994) 173.
- 32) We define the charging energy  $E_c$  as the energy required to generate fully dissociated positively and negatively charged grains.
- 33) D. V. Averin and Yu. V. Nazarov: *Single Charge Tunneling*, edited by H. Grabert and M.H. Devoret, p.224, (Plenum Press, Ney York, 1992).
- 34) D. V. Averin, A. A. Odintsov, and S. V. Vyshensky: J. Appl. Phys. **73** (1993) 1297.
- 35) D. V. Averin: Physica **B194-196** (1994) 979.
- 36) The conductance between the large grains in Fig. 4(b) is proportional to  $\Delta V (\propto n)$  and the density of the conduction path normal to the current direction ( $\propto 1/n^2$ ), so that  $f(n) \propto 1/n$ .
- 37) M. Ohnuma, K. Hono, E. Abe, H. Onodera, S. Mitani, and H. Fujimori: J. Appl. Phys. **82** (1997) 5646.